*International Research Journal of Environmental Sciences*_____ ISSN 2319–1414
Vol. **10(2),** 52-63, April **(2021)** *Int. Res. J. Environmental Sci.*

Study of the adsorption of glycine by two local clays of Congo Brazzaville

Kouhounina Banzouzi Merline lady[1], Diamouangana Mpissi Flora Zita[1,2], Ifo Grace Mazel[1], Bibila Mafoumba Jean Claude[1] and Moutou Joseph –Marie[1,2]

[1]Laboratoire de Chimie minérale et Appliquée, Faculté des sciences et Techniques, University Marien Ngouabi, B.P. 69, Brazzaville, Congo
[2]Ecole Normale Supérieure, University Marien Ngouabi, B.P. 69, Brazzaville, Congo
florajullie@gmail.com

Available online at: www.isca.in, www.isca.me
Received 2nd November 2020, revised 8th February 2021, accepted 23rd March 2021

Abstract

In this work, we are studying the interaction of two Congolese clays with glycine, the clays soils collected in the localities of Missafou and Mouyondzi. The two adsorbents have been characterized beforehand. Mineralogical analysis is determined using different techniques (DRX, IR, ATD, ATG, DTG). Among the physicochemical properties, the chemical composition is obtained by ICP-AES, the CEC is evaluated by the Metson method. The surface properties are derived from the nitrogen adsorption / desorption isotherm on the MISA-B and MOU samples. The geotechnical properties (particle size and Atterberg limits) were measured. The results of the characterization showed that Talc is the predominant species in Missafou clay. Batch mode adsorption tests have shown us that the adsorption capacity of glycine on Mouyondzi clay is better. Langmuir's model better describes these adsorption isotherms.

Keywords: Clay, glycine, adsorption.

Introduction

Clay has an importance in the lives of men. Indeed clays are used in several areas. We can cite its use in the cultivation of land, in the rehabilitation of structures and in the resolution of environmental problems[1]. Its wide use derives from its properties. In addition, clay-organic matter interactions have been the subject of numerous studies. In this context, the following objectives are pursued: i. Given the fact that human activities cause a large amount of organic matter in the environment, in particular in aquatic environments (surface water and groundwater), the elimination of this sometimes leads to the use of raw or modified clays as adsorbents[2,3]. ii. Clays, always related to their adsorbent properties, are used as catalysts in several chemical reactions (alkylation, cracking, dehydrogenation, epoxidation, etc.)[2].

A study on the adsorption of enzymes on phyllosilicates and other minerals in the soil showed a high affinity between the adsorbate and the adsorbent[4]. Enzymes can be obtained before or after degradation of biota (living microorganism and plant roots). Ordinary, biota cannot adsorb large molecules directly from nature. Overall, membrane transport mechanisms are unique to each species and identity amino acids, sugars and nucleotides which are universal biological monomers. Among the functions that enzymes perform, we can cite the fact that they convert large molecules into small molecules which in turn are recognized and adsorbed by membrane transport mechanisms. The strong adsorption of enzymes on the mineral phase of the soil induces its irreversibility, thus leading to mobility, monitoring and catalytic activity of these enzymes. Stotzky indicates that the activity of catalase (an enzyme responsible for the fragmentation of macromecules) linked to a montmorillonite homoionized to certain cations was four times greater than that of free catalase[5]. Moreover, Kitadai et al were interested in the polymerization of glycine on mineral surfaces (oxides and clay minerals). And they indicated the catalytic activity of the latter[6]. A number of clay soils extracted from Congolese soil have been characterized[7-9]. Mouyondzi clay was characterized and kaolinite was found to be the dominant species[10]. This work consists of studying the interaction of two Congolese clays with glycine in order to determine the affinity of these soils with glycine. Specifically we intend to characterize one of the chosen materials.

Materials and methods

Location and description of sampling sites: Missafou and Mouyondzi are two districts located in the department of Bouenza (in the south of the Republic of Congo). The geographic coordinates recorded in Table-1 enabled us to locate the sampling sites.

Table-1: Geographic coordinates.

Sample	Latitude	Longitude	Altitude
Missafou	9518750	0373551	235 m
Mouyondzi	9518750	0382155	410 m

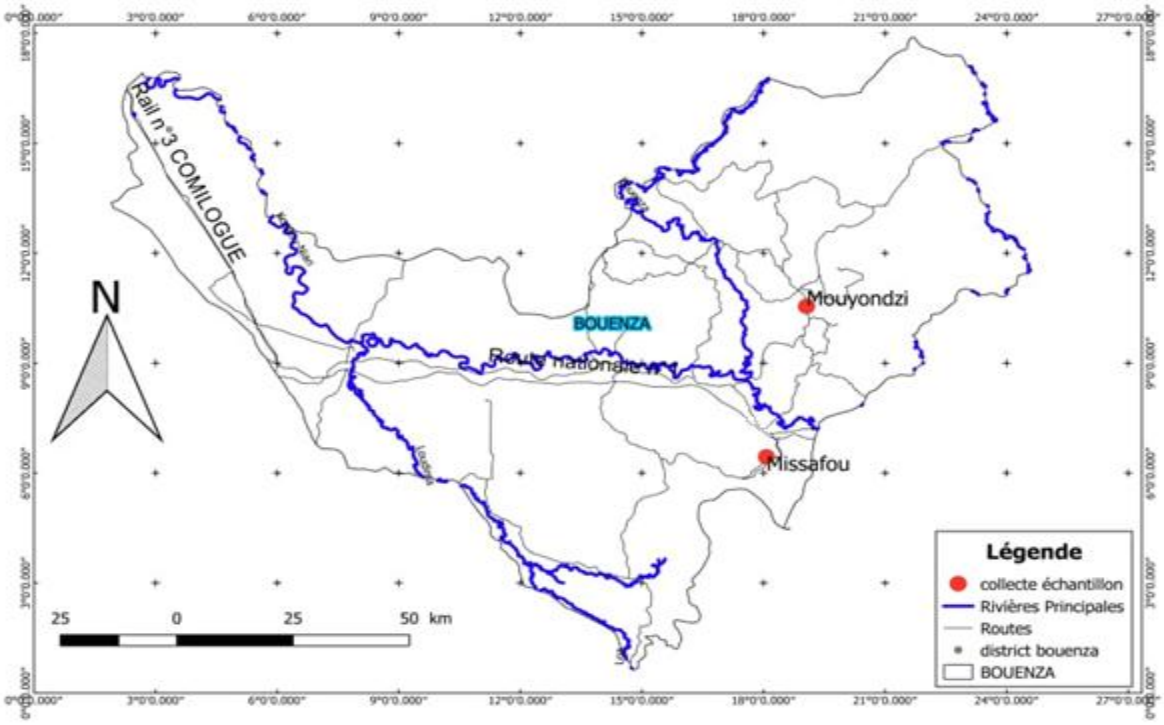

Figure-1: Location of sampling sites[11].

Mineralogical characterization of Missafou clay: The X diffractogram was recorded on the raw sample at the Bordeaux condensed matter chemistry institute (ICMCB) in France using a Philips brand diffractometer using a copper anticathode (λ = 1.54054Å). The angular range varies from 5° to 80°. The diffractogram processing was carried out, using the Full proof software[12].

The IR spectrum was carried out at the Laboratory of Environment and Mineralurgy (LEM) of Nancy with a Fourier transform infrared spectrometer of the BRUKER IFS 55 brand equipped with a broad band detector of the type MCT (mercury and cadmium tellurium) cooled to 77K and a diffuse reflection accessory (Herrick Corporation) with KBr as a matrix. The acquisition is carried out on 200 scans (approximately 1mn 30) and the spectral resolution is $2cm^{-1}$.

The thermal analyzes were carried out at the Ceramic Technologies Transfer Center (CTTC) in Limoges (France). The Differential thermal (DTA) and gravimetric analysis (GTA) were carried simultaneously out with a device from Setaram Scientific and Industrial Equipment, Setsys 24 series coupled with thermobalance and the mass spectrometer THERMOSTAR between 20 and 1250°C under air purge. The speed of heating being 10˚C/min.

Geotechnical characterization: The ATTERBERG limits are determined in the soil analysis laboratory of the building and public works control office (BCBTP) in Brazzaville (Republic of Congo) according to the norms NF P 94-051 and 94-052[13].

Size of the different fractions of the material was given by the method described by the norm NF X 31-107 out in Soils Arras Laboratory (LAS)[14].

Chemical characterization: mass percent of the elements oxide was determined out at Petrographic and Geological Center of Research (PGCR) of Nancy in France. The analysis was carried by induced coupled plasma atomic emission spectrometry (ICP-AES)[15]. The determination of free iron and aluminum in our sample was carried out according to two methods (Mehra Jackson method and Tamm method) at the Arras Laboratory[16,17].

The organic carbon (C) and total nitrogen (N) which constitute the organic matter determined by method described by NF ISO 10694 and 13878 at the Arras Laboratory[18].

Surface properties: The adsorption / desorption isotherm was obtained using an automatic point-to-point gas adsorption volumetric apparatus, at the Laboratory of Environment and Mineralurgy (LEM) in Nancy (France). From this isotherm, the specific surface is evaluated using the BET method[19].

Cation exchange capacity (CEC) is performed according to the Metson method at the Arras Laboratory[20].

The method used is described in the AFNOR NFX31-130 standard[21]. The characteristics of mouyondzi clay are collated in Table-1[10]

Glycine adsorption kinetics and isotherm: The kinetics and isothermal absorption of glycine by the clays of Missafou and Mouyondzi were carried out by the batch method in the Laboratory of Applied Chemistry Mineral (LaCMA) of Marien NGOUABI University at the Faculty of Sciences and Technicals. The contact time was determined by mixing 1g of clay with 20mL of glycine solution at 0.01mol/l. the suspension obtained is stirred at different times in intervalle from 5min to 40 min at room temperature. The mixture is then centrifuged for 15 minutes at 3000rev / min then the supernatant is immediately assayed by a UV-visible spectrophotometer of zuzy brand at a wavelength of 560nm after reaction with ninhydrin at the Laboratory of Cellular and Molecular Biology (LBCM) of Marien NGOUABI University at Sciences Faculty and Technicals of Brazzaville in Congo. To carry out the adsorption isotherms, different dilutions of the glycine solution prepared from a stock solution of 0.01mol / l are carried out with the same mass of clay. The mixtures are stirred for a period determined by the kinetics. The supernatant is separated by centrifugation at 3000rev/min for a time of 15 min. The residual glycine concentration is determined by UV-VIS spectrophotometry at a wavelength of 560nm after reaction with ninhydrin.

Results and discussion

X-ray diffraction: The determination of the structural phases of raw Missafou clay by X-ray diffraction is given in Figure-2.

Observation of this diffractogram identified three clayey species: Talc, kaolinite and chlorite. The impurities associated with these minerals are goethite, dolomite, quartz and anatase. The characteristic peak of talc ($Mg_3Si_4O_{10}(OH)_2$) at 9.3Å is most intense in the diffractogram. We find that the other three peaks of talc namely the peaks at 4.55Å, 3.14 and at 1.85Å are as narrow and well resolved as the peak at 9.3Å, indicating good crystallinity. The very weak and broad peak at 7.13Å and its harmonic at 3.57Å (1207 intensity) indicate traces of kaolinite or chlorite. Quartz can be identified by the peak at 1.98Å. Dolomite would correspond to the peak at 2.58Å, goethite at the peak at 4.22Å. The peak at 3.4 leads us to consider the presence of anatase.

Chemical analysis: The results are shown in Table-3.

Table-2: Characteristics of Mouyondzi clay[10].

Granulometry	< 2 µm	2-20 µm	20-50 µm	50-200 µm	200-2000 µm
	65%	20.9%	8.1%	3.6%	2.4%
Organic matter	Organic carbon	Total nitrogen	C/N	Organic matter	
	0.485g/kg	0.047g/kg	10.32	0.839g/kg	
Atterberg limits	Liquidity limit	Plasticity limit	Plasticity index		
	51.2	22.3	28.9		
CEC	8.66 cmol+/kg				
Extractableiron	Tamm iron 0.05g/100g	Mehra Jackson iron 0.098 g/100g			
TammAl	Tamm Al¨0.059g/100g	MehrajacksonAl0.085g/100g			

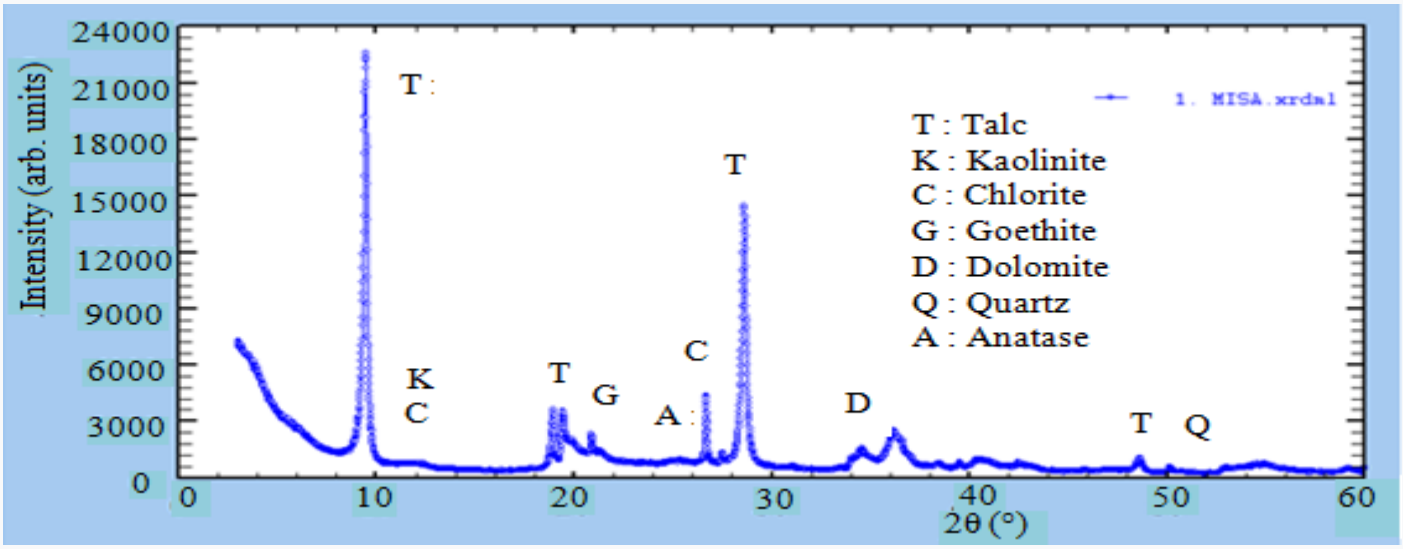

Figure-2: Spectrum of raw MISA-B clay.

Note that MISA-B consists essentially of silica (56.43%) and magnesia (22.22%). The value of the SiO_3 / Al_2O_3 ratio is equal to (8.42). This explains by the high content of silica, the relatively high content of magnesia corroborates the mineralogical composition of MISA-B namely that it is composed of mineral phases source of MgO. The relatively high Fe_2O_3 content (2.84%) would come mainly from the goethite (FeO(OH)) observed on the X spectrum of the MISA-B sample. the anatase revealed by XRD corroborates the presence of titanium albeit very weak in the chemical analysis.

The Table-4 gives us some chemical properties of the MISA-B sample. The measured low MISA-B CEC is 7.89cmol + / 100g. In fact, talc hardly presents any substitution in the sheets. As the surface load is therefore low, talc does not have a high adsorption capacity[22]. To this is added the significant presence of goethite and also quartz attenuating the CEC from talc, which would explain the value of the CEC observed.

The percentage of free iron is 79.47%. It is to this free iron that certain properties of the soil are attributed, such as sometimes the structure; but also and above all the color. This iron is involved in oxides and hydroxides (hematite and goethite), complexed in organic matter and amorphous (ferrrihydrite)[15]. Iron bound to organic matter is very low (0.025g/100g)[14]. This result is in an agreement with that of organic matter in this soil (11.9g/kg), because in this case of generally unstable buildings the metal only exists in rather small quantities. This percentage of free iron shows that a large part of the iron is involved in the hydroxides; goethite as confirmed by the DRX.

Aluminum bound to organic matter would exist in low amounts considering the Tamm aluminum content. On the other hand, the aluminum present in the free oxides would be very negligible given that the difference between the rate of Al Tamm and the rate of Al Mehra Jackson is small.

Infrared spectroscopy: The Figure-3 gives us the infrared spectrum of MISA-B. The XRD study of the MISA-B sample revealed the presence of talc. A trioctahedral T-O-T mineral, the octahedral layer is occupied by magnesium atoms. Each OH hydroxyl group is therefore linked to three magnesium atoms. The observation of an intense band at 3676cm^{-1}, characteristic of Mg_3O-H valence vibrations, confirms the presence of talc[23]. On one hand, the band has 3700cm^{-1} could be linked to the presence of kaolinite. Considering the greater intensity of the band at 3623cm^{-1} compared to that at 3700cm^{-1}, it is less likely that the two bands are considered to be kaolinite. In fact, in kaolinite the two bands have practically the same intensity. Nkoumbou C and et al[24]. Indicate that the 3623cm^{-1} band characterizes ion clusters (3Fe-OH). So we can think of a substitution of magnesium by iron. On the other hand, some authors indicate that the MgO-H mode of elongation in Mg $(OH)_2$ brucite shows a band at 3698cm^{-1}. In this case, the band at 3700cm^{-1} would correspond to brucite. And like Frost R. and Kloprogge, the 3620cm^{-1} band would be associated with kaolinite. Given the band width at 3623cm^{-1} and the fact that brucite is not observed on the XRD spectrum, we are looking at the presence of ion clusters (3Fe-OH). The wide band around 3403 and 1647cm^{-1} correspond at the presence of water[25]. Bands at 2926 and 2856cm^{-1} attributable to organic matter[26]. XRD spectrum revealed the presence of dolomite. The presence of dolomite is confirmed by the band at 1458cm^{-1}. Bands at 1111 and 1050cm^{-1} are assigned to Si-O stretching vibration mode. Band at 997cm^{-1} can be attributed to the Si-O-Si vibrationin talc would indicate the possibility of substitution of silicon by aluminum or iron in the tetrahedral layer. This is because substitutions generally result in a lowering of the frequency. Brindley and Brown report that it is possible to incorporate up to 4.0% alumina in talc. The bands at 914, 798 and 780cm^{-1} show the presence of quartz which has been identified in the XRD spectrum[27]. The band at 755cm^{-1} corresponds at kaolinite (Si-O). The strong band at 667cm^{-1} is a characteristic of the deformation mode (Si-O) in a trioctahedral mineral.

Table-3: Chemical Analysis of MiSA-B.

Oxide	SiO_2	Al_2O_3	Fe_2O_3	MnO	MgO	CaO	Na_2O	K_2O	TiO_2	P_2O_5	PF	Total
Content(%)	56.43	6.7	2.84	0.07	22.22	0.36	0.08	0.4	0.22	⟨ LD	10.46	99.78

Table-4: Chemical properties of Missafou sample.

Organic matter	Organic carbon	Total nitrogen	C/N	Organic matter
	6.86g/kg	0.689g/kg	9.96	11.9g/kg
CEC	7.89 cmol+/kg			
Extractableiron	Tamm iron 0.025g/100g		Mehra Jackson iron 1.58 g/100g	
TammAl	Tamm Al 0.08g/100g		Mehrajackson Al 0.251g/100g	

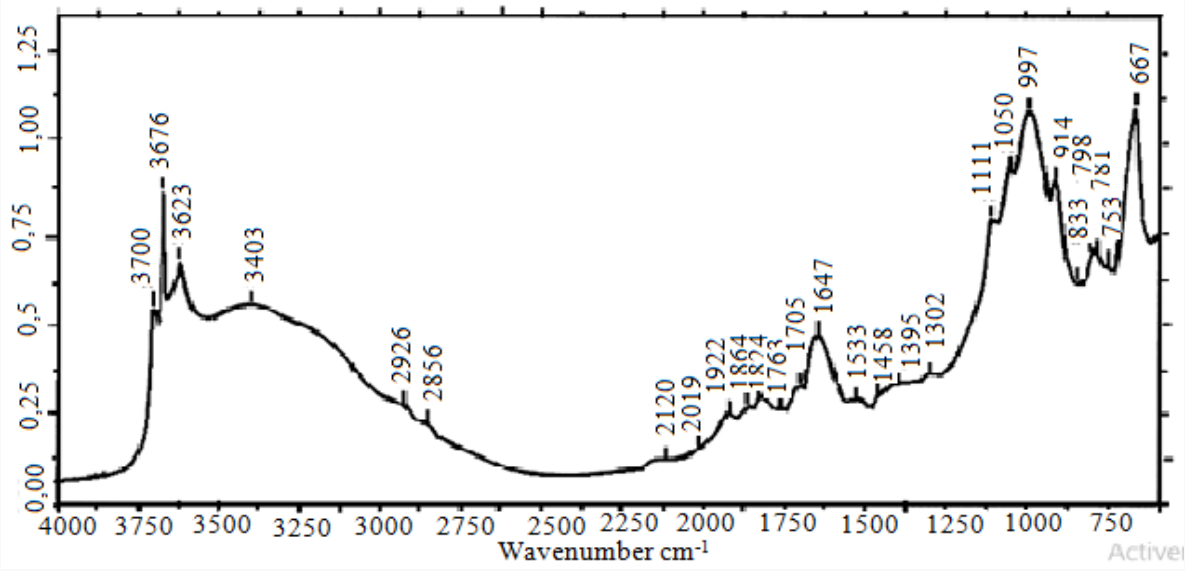

Figure-3: IR spectrum of MISA-B.

Mineralogical assessment: The percentages of kaolinite, talc, quartz and dolomite in the MISA-B sample are calculated using the following relationship[28]:

$$T(a) = \sum_{i}^{n} Mi.Pi(a)$$

Which: $T(a)$: Percent of the element oxide a in the sample; T(a) is given by chemical analysis; Mi: Content (in%) of mineral i in the material and containing the element a; Pi(a): percent of the element a in the sample i.

The procedure for calculating mineralogical balance is such that: i. Kaolinite is determined by the percentage of Al_2O_3 given by chemical analysis, ii. The MgO content allows calculating the percentage of dolomite and talc. iii. Quartz is determined by the difference between the SiO_2 contentin the chemical analysis and the proportions in SiO_2 corresponding to kaolinite and talc.

The results of the mineralogical balance are given in Table-5.

Table-5: Mineralogical compositions in MISA-B (% by mass).

Minerals	Mineral percentage (in%)
Kaolinite	17,18
Talc	53,93
Quartz	14,38
Dolomie	22,87

Differential and gravimetric thermal analyzes: The differential thermal analysis (ATD), thermogravimetric (ATG) and differential thermogravimetric (DTG) analysis curves are given respectively in Figures-4, 5 and 6. The ATD shows 5 endothermic peaks and two exothermic peaks.

A first very broad endothermic peak in the temperature range from ambient up to 200°C. It corresponds to a first mass loss of 3% caused by the departure of water adsorbed on the surface of the clay minerals constituting MISA-B. Adsorbed water can be removed by simple heating to temperatures ranging from 80 to 300°C[29]. Between 450°C and 520°C, the second equally weak endothermic peak, the maximum of which is 500°C, which can be attributed to the start of the water of constitution (dehydroxylation of the structure)[29]. The third endothermic peak between 550 and 650°C, also weak, the maximum of which is located at 600°C, is attributed to the dehydroxylation of the hydroxide sheet of the chlorite which causes a loss of mass of 2%. The fourth endothermic peak between 800 and 931°C and particularly strong, the maximum of which is located at 905°C, reflects the dehydroxylation of the talc which causes a mass loss of 3.5% estimated from the ATG curve, between 900 and 1025° C, the last endothermic peak corresponds to the destruction of the talc sheet ($Si_4Mg_3O_{10}(OH)_2$) which turns into clinoenstatite ($MgO.SiO_2$) according to equation[30].

$$\underset{\text{Talc}}{4SiO_2\ 3MgO,\ H_2O} \longrightarrow \underset{\text{Clinoenstatite}}{3MgO.\ SiO_2} + \underset{\text{Cristobalite}}{SiO_2} + H_2O$$

The first exothermic peak around 350°C associated with a mass loss of around 1.3% revealing the presence of organic matter, ferrihydrite and/or iron or even aluminum oxyhydroxides. Based on the results of XRD analysis, the presence of goethite can explain this transformation between 250°C and 350°C, which would correspond to its dehydroxylation[31].

$$2FeO(OH) \rightarrow Fe_2O_3 + H_2O$$

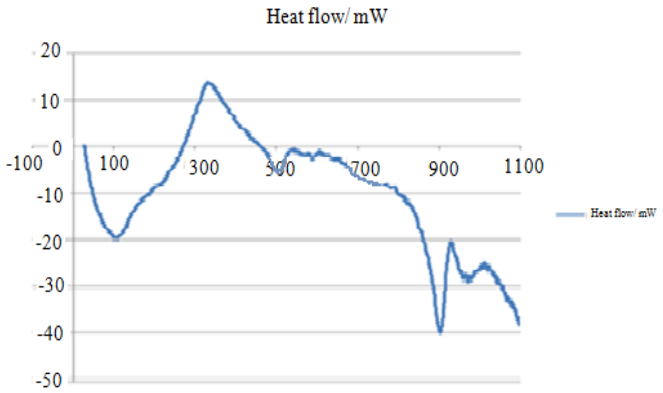

Figure-4: ATD MISA-B thermogram.

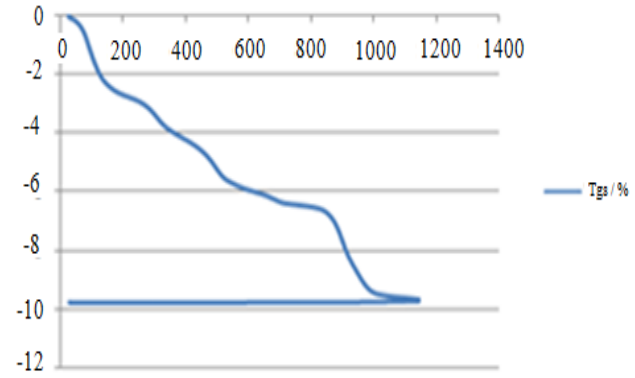

Figure-5: TG curve of MiSA-B.

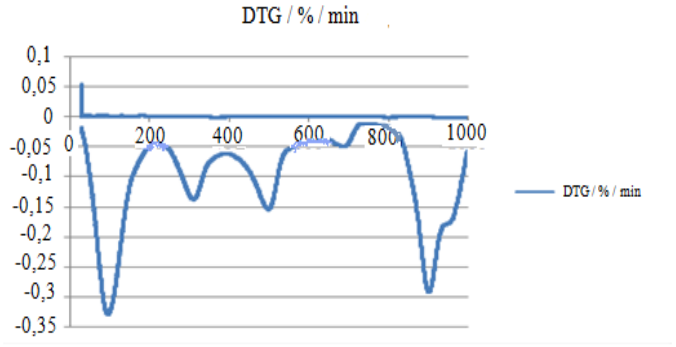

Figure-6: DTG curve of MiSA-B.

Geotechnical properties: Table-6 gives us the results of the Atterberg limits.

Table-6: Atterberg limits results.

Sample	Liquidity limit	Plasticity limit	Plasticity index
MISA-B	41	23	18

The Atterberg limits obtained allow MISA-B to be placed in the Casagrande abacus[32].

These plasticity parameters allowed us to identify the nature of our clay, using the Casagrande abacus (Figure-7). MISA-B is located just above line A in the hatched area which indicates illite, this indicates that MISA-B does correspond to a type (2: 1) phyllosilicate.

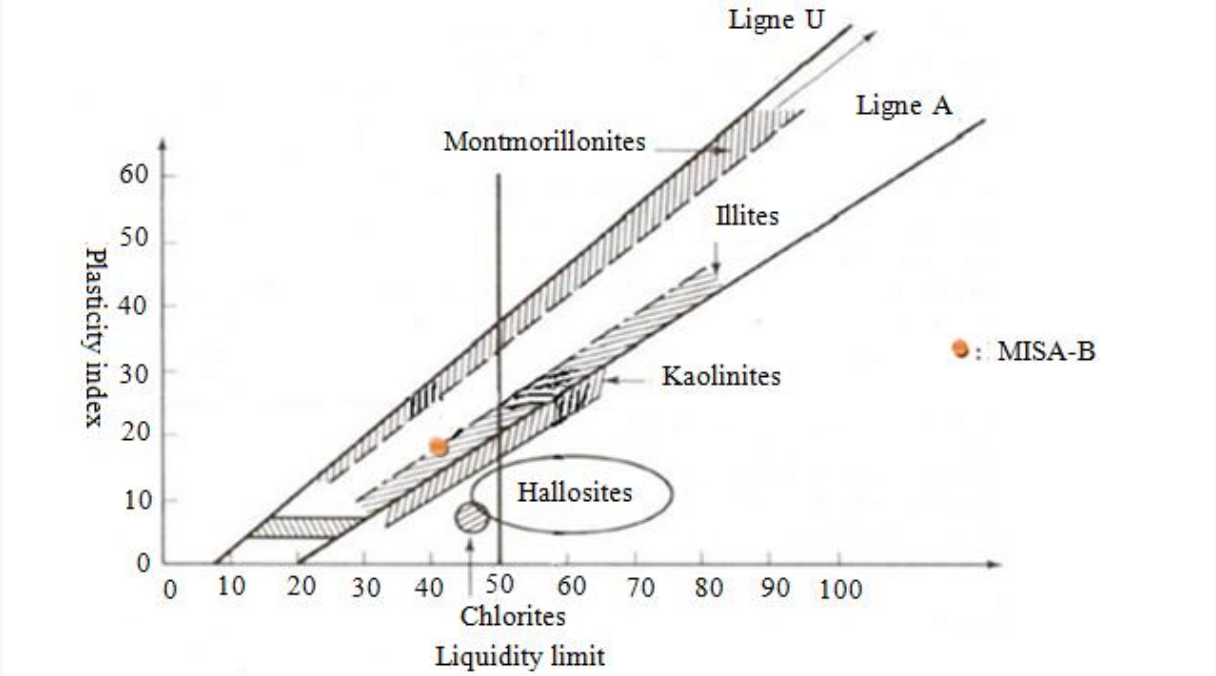

Figure-7: Positioning of MISA-B in the Casagrande chart.

Table-7: Particle Size analysis.

Sample	< 2 µm	2-20 µm	20-50 µm	50-200 µm	50-200 µm
MISA-B	36%	10.3%	5.2%	9.2%	39.3%

The grain size composition gives this soil a clay texture. The fine fraction (<2µm) responsible for the plasticity justifies the mean values of the Atterberg limits. The results of the particle size analysis allowed us to position MISA-B in the texture triangle[33]. The percentages in clay (36%), silty (15.5%), and sandy (48.5) fractions allow us to attribute to MISA-B a sandy clay texture. These results are compatible with their plasticity.

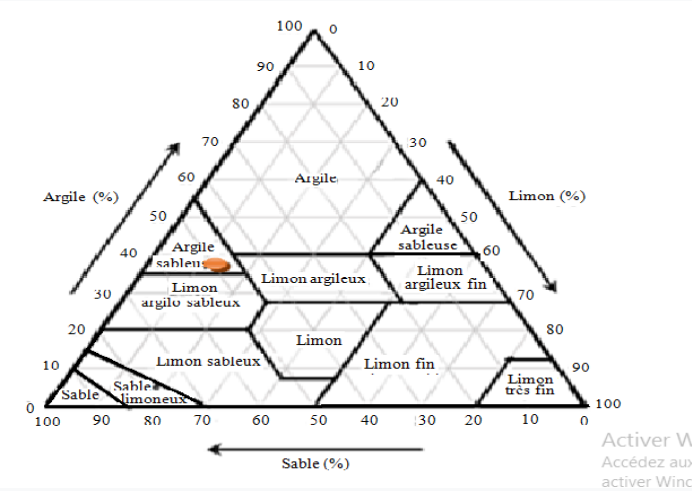

Figure-8: Texture triangle from Survey Manual Threshold.

Plasticity index and activity: the activity of clays is calculated by the following relationship[34]:

$$A = \frac{Ip}{C}$$

Which, Ip: Plasticity index, C: Percent of elements less than two microns.

The Table-8 presents the results on the plasticity indices and the activities of the samples.

Table-8: Results on the plasticity indices and the activities of the samples.

Sample	Plasticity index	Percentage of clay	Activity
MISA-B	18	36	0,5
MOU	28,9	65	0,44

The activity values of the MISA-B and MOU samples are close to each other. MOU is formed from kaolinite; MISA-B is of the illite type (type 2: 1 phyllosilicate).

Specific surface: The Figure-11 shows the adsorption / desorption isotherm of MISA-B and MOU.

The adsorption isotherms obtained are type IV according to the Brunauer classification[35]. This isotherm is obtained with mesoporous adsorbents in which capillary condensation occurs[36]. The hysteresis in these isotherms is of type H3. Type H3 is quite rare and corresponds to slit pores of non-constant section. The H3 hysteresis loop is observed when the adsorbent forms aggregates[37]. For both samples, there is a gradual reduction in hysteresis but slower for MISA-B as the relative pressure decreases. This indicates that the MISA-B sample has more mesopores than the MOU sample. The numerical data deduced from these isotherms reveal that the MOU sample has a pore volume of 110cm^3/g; the MISA-B sample has a pore volume of 45.2cm^3/g.

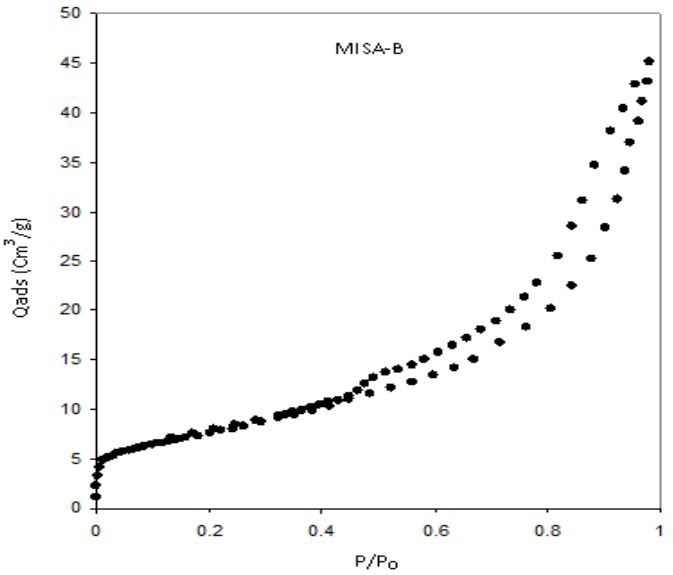

Figure-9: Adsorption / desorption isotherm of N_2 on MISA-B.

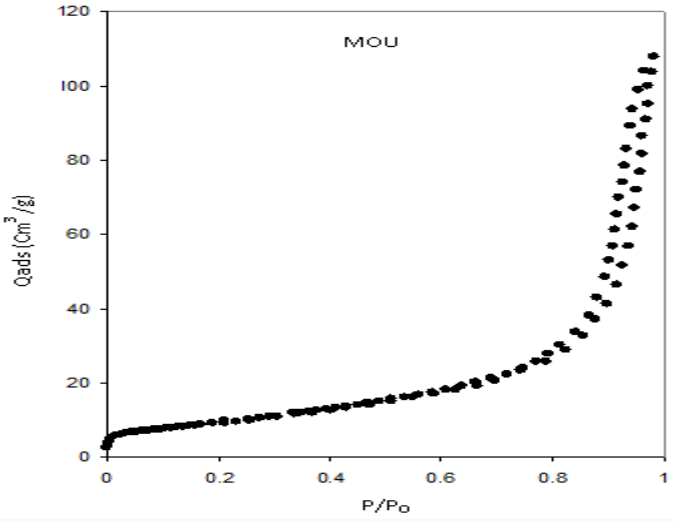

Figure-10: Adsorption / desorption isotherm of N_2 on MOU.

From these isotherms the value of the specific surface was deduced. By the t-plot method, the internal surface could be measured.

Table-7: Value of the specific surface.

MISA-B	Totale specifiq Surface 27,3 m^2/g	External specifiq Surface 26 m^2/g	Internal specifiq Surface 1,1m^2/g
MOU	Totale specifiq Surface 33,7 m^2/g	External specifiq Surface 32,9 m^2/g	Internal specifiq Surface -

Kinetics and Isothermal adsorption: Kinetics of adsorption by Missafou and Mouyondzi: The Figures-11 and 12 show the adsorbed amounts of glycine in function of contact time respectively by Missafou and Mouyondzi clays. The evolution in adsorbed quantity of glycine in function of contact time on missafou and mouyondzi clays presented by Figures-11 and 12 shows that in the case of missafou, the glycine retention process takes place in three fairly distinct. A first, very fast during the first 5 minutes. This would correspond to a fixation of the glycine on the surface of the clay which can be explained by the great affinity of the clay vis-à-vis the adsorbate used[38]. The second shows a slow increase in the adsorbed amount of glycine, characteristic of the diffusion process through the sheets.

This quantity continues to increase throughout the reaction time. This suggests that the phenomena of surface fixation could be prolonged even during the second reaction phase. The balance is reached after 25 minutes of contact time when all the sites become occupied.

In the case of Mouyondzi clay, the figure shows that the retention process at the level of the first phase is rapid up to approximately 20min. This suggests that there is also fixation of glycine on the surface of this clay. In the second phase there is a slow increase in the glycine elimination yield until the equilibrium time (40min).

The comparison of the results indicates that in the same mass of clay, greater retention is obtained for Missafou (10.83mg/g for MISA-B and 8.76 for MOU). Indeed, a large proportion of glycine (more than 50% of the amount introduced) is absorbed by Missafou clay after the first 10 minutes. This proportion does not exceed 30% for Mouyondzi clay. This difference between the adsorption capacities of the two clays is probably linked to their structure because, according to the work carried out by Moutou et al, the mineralogical characterization revealed that the clay of mouyondzi is kaolinitic (type 1/1) [10]. The results of spectrum of raw MISA-B (Figure- 2) revealed the presence of talc for Missafou (type 2/1). Similar results have also been observed by Nouzha BOUZIANE, using clays of different structure[39].

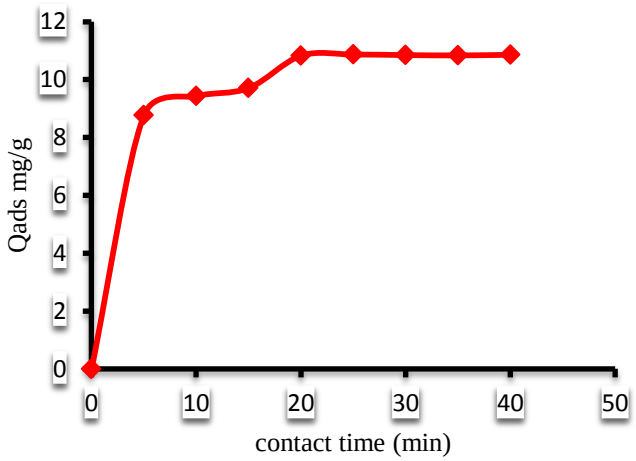

Figure-11: Kinetic study of glycine adsorption on MISA-B.

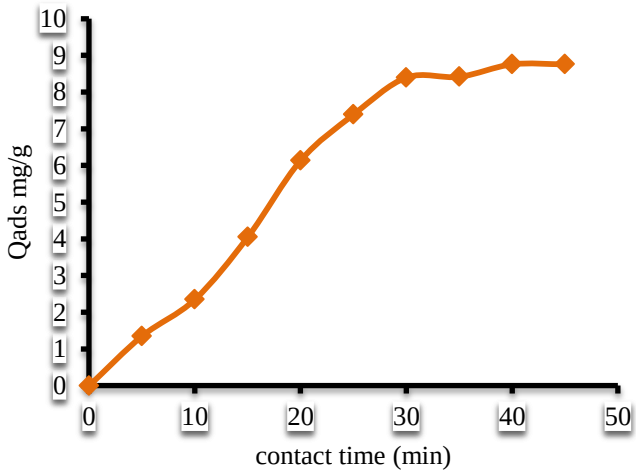

Figure-12: Kinetic study of glycine adsorption on MOU.

Isothermal adsorption by Missafou and Mouyondzi: The Figures-13 and 14 give us the isothermal adsorption of glycine by Mouyondzi and Missafou clays obtained by plotting the adsorbed quantity Qa (mg/g) as a function of the concentration at equilibrium Ce (mg/l). The influence of the concentration at equilibrium on the amount of adsorption of MISA-B and MOU clays shows an increase in the amount of glycine adsorbed as a function of the increase in concentration at equilibrium. This behavior may be due to the presence of a large amount of glycine in solution, which would imply massive adsorption within the materials thus causing an increase in the amount of adsorption of MISA-B and MOU. The adsorption isotherm of MISSA (Figures-13) is of type S1, which indicates that the adsorbed molecules of glycine favor the adsorption of other molecules which will be done after[40]. She can be explained by the fact that the molecules attract each other by weak intensity forces called Van Der Waals forces and gather in islands in which they are packed against each other [41].

In the case of the Mou clay isotherm (Figure-14), it is of type L, this form of isotherm expresses the flat adsorption of bi-functional molecules. In this case the adsorption of the solvent is low and that of the solute on the solid is done in a monolayer[40]. The adsorbed amount of glycine in Missafou clay is 9.12mg/g while that of Mouyondyi is 10.71mg/g. These results are in agreement with the presence of a specific surface and a higher percentage of fine particles for mouyondzi.

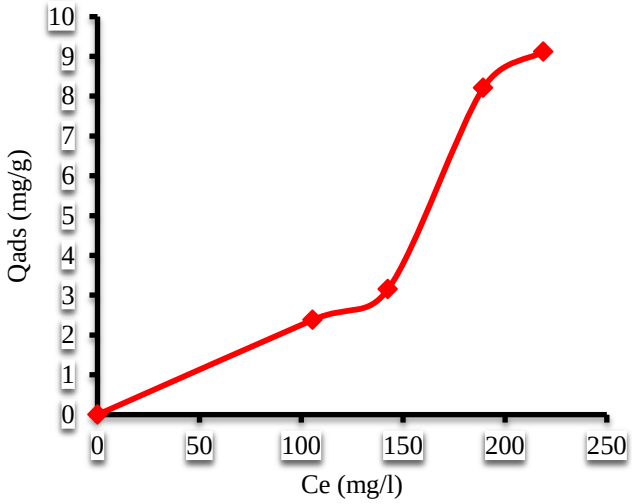

Figure-13: Adsorption isotherm on MISA-B.

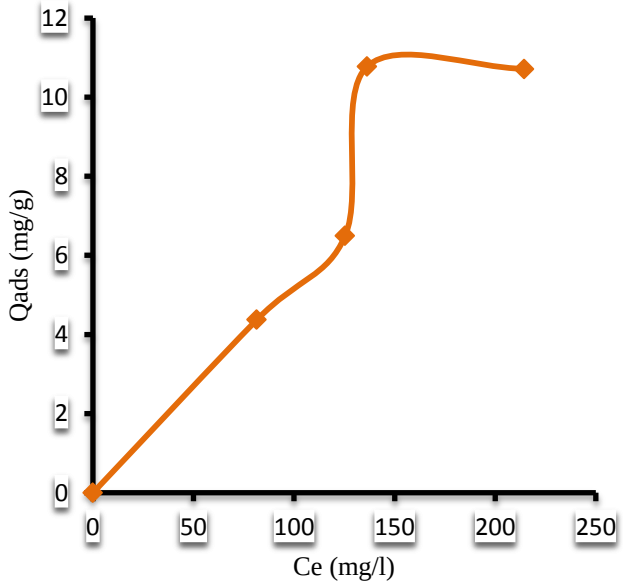

Figure-14: Isothermal adsorption on Mou.

Modeling of the adsorption isotherms: Figure-15 and 16 shows the Langmuir model and Figure-17 and 18 shows the Freundlich model.

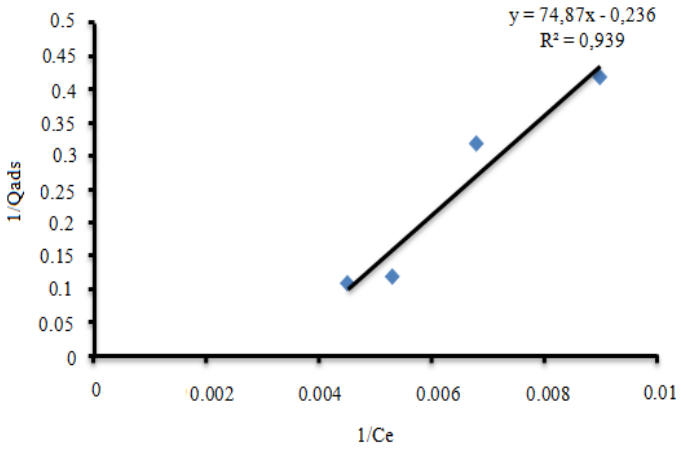

Figure-15: Linear representation of the langmuir relation for glycine on MISA-B.

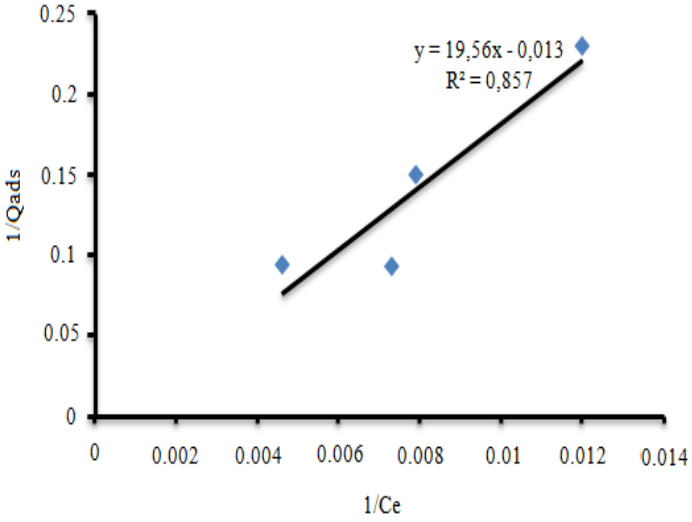

Figure-16: Linear representation of the langmuir relation for glycine on MOU.

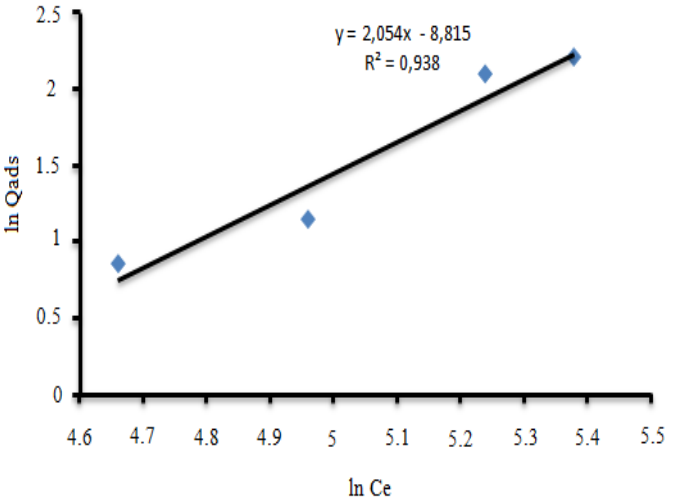

Figure-17: Linear representation of the Freundlich relation for glycine on MISA-B.

Table-8: Different Langmuir and Freundlich coefficients Obtained from experimental results, for glycine on Mouyondzi and Missafou clays.

Materials clayey	Parameters of Langmuir			Parameters of Freundlich		
	Qmax (mg/g)	K_L (L/mg)	R^2	1/n	K_F	R^2
MISA-B	4,23	0,003	0,939	2,054	0,00014	0,938
MOU	76,9	6,63	0,857	0,950	0,07	0,760

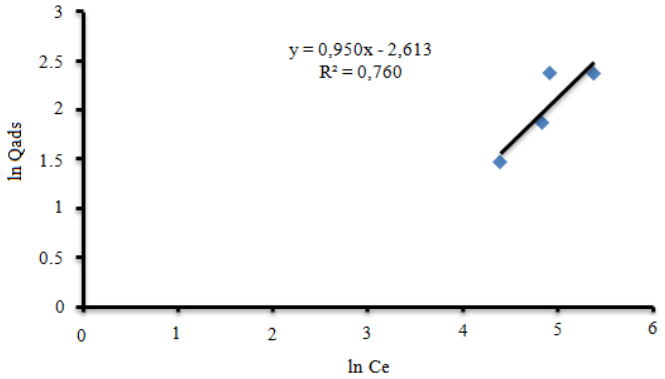

Figure-18: Linear representation of the Freundlich relation for glycine on MOU.

The parameter 1/n which indicates the intensity of the adsorption is 2.054 for MISA-B and 0.950 for MOU. It has been reported in the literature that adsorption is favorable for values of n>1 [35]; this value is 0.52 for MISA-b and 2.08 for MOU, which allows us to say that the adsorption of glycine is favorable with Mouyondzi clay. This confirms the maximum adsorption capacity Qmax which is 76.9mg/g for Mouyondzi. The distribution coefficient of Freundlich K_F is relative to the total sorption capacity of the solid, it is 0.00014 for MISA-B and 0.07 for MOU. K_L which is the thermodynamic constant of the adsorption characteristic adsorption equilibrium is 0.003 for MISA-B and 6.63 for MOU and R which is the correlation coefficient are all close to unity; 0.925 with the Langmuir model and 0.871 with the Freundlich model. This induces a great affinity between the particles of glycine and Mouyondzi clay. Taking into account the two models, the adsorption of glycine on MISA-B and MOU is better described by the isotherm of LANGMUIR.

Conclusion

The principal goal pursued in this work was to evaluate in the adsorption capacity of two clay soils (Missafou and Mouyondzi) in the presence of the glycine. To achieve this goal, we used several techniques. The characterization of the clay of Missafou was made using the following methods: DRX, IR, ATD, ATG, DTG, CEC, AG and SS. The kinetics and the adsorption isotherm of glycine was carried out by the batch method. Two models were used for modeling: adsorption Isothermal, Langmuir and Frendlich models. Mineralogical analysis of Missafou clay gave a preponderance of Talc with a very intense peak at d = 9.3Å. These results are confirmed by those obtained with infrared which showed the characteristic bands of Talc. ATD showed an endothermic peak (900-1025°C) corresponding to the destruction of the talc sheet ($Si_4Mg_3O_{10}(OH)_2$). The particle size analysis gave us a fine fraction percentage of 36, which gives the Missafou soil a sandy clay texture with a plasticity of 18. The BET method revealed a specific surface area of 27.3m^2/g and 33.7m^2/g for a cation exchange capacity of 7.89cmol + / Kg and 8.66cmol + /kg respectively for MISA-B and MOU. Glycine adsorption equilibrium is reached in 25 minutes of adsorbate-adsorbent contact time for Missafou clay and 40 minutes for Mouyondzi clay. The adsorption isotherm is type S1 for Missafou and L for mouyondzi. By comparing these two clays, we were able to conclude that Mouyondzi clay adsorbs better than that of Missafou with adsorption quantities of 10.71mg/g and 9.12mg/g respectively for Mouyondzi and Missafou.

References

1. Konta, J. (1995). Clay and man: Clay raw materials in the service of man. *Applied Clay Science*, 10(4), 275-335.
2. Bouras, O. (2003). Propriétés adsorbantes d'argiles pontées organophiles: synthèse et caractérisation. Thèse de doctorat, Université deLimoges France, 1- 162.
3. Errais, E. (2011). Réactivité de surface d'argiles naturelles. étude de l'adsorption de colorants anioniques. Thèse de doctorat, Université de strasbourg, 1-210.
4. Quiquampoix, H., Servagent-Noinville, S. and Baron, M-H. (2002). Enzyme Adsorption on Soil Mineral Surfaces and Consequences for the Catalytic Activity. Marcel Dekker, Inc. 285-306. https://doi.org/10.1201/9780203904039.ch11.
5. Stotzky, G. and Pramer, D. (1972). Activity, ecology, and population dynamics of microorganisms in soil. *CRC Critical Reviews in Microbiology*, 2(1), 59-137. https://doi.org/10.3109/10408417209108388.
6. Kitadai, N., Oonishi H., Umemoto K., Usui, K.F. and Nakashima, S. (2017). Polymérisation de la glycine sur les minéraux oxides. *Orig life Evol Biosph*, 47(2), 123-143, https://doi.org/ 10. 1007/s11084-016-9516-z.
7. Diamouangana Mpissi, Z.F., Moutou, J.M., Matini, L., Mongo Oladzon, M.F. and Kouhounina Banzouzi, L. M.

(2019). Synthesis of an inorgano-clay complex from loukolela clay and application in the adsorption of humic matter. *Int. Res. J. environment Sci*, 8(3), 12-20.

8. Moutou, J.M., Bibila Mafoumba, C., Matini, L., Ngoro Elenga, F. and Kouhounina, L. (2018). Characterization and evaluation of the adsorption capacity of dichromate ions by a clay soil of impfondo. *Res. J. Chem. Sci.*, 8(4), 1-14.

9. Moutou, J.M., Mbedi, R., Elimbi, A., Njopwouo, D., Yvon, J., Barres, O. and Ntekela, H.R. (2012). Mineralogy and Thermal Behaviour of the Kaolinitic Clay of Loutété (Congo-Brazzaville). *Research Journal of Environmental and Earth Sciences*, 4(3), 316- 324

10. Moutou J. M., Foutou P. M., Matini L., Banzouzi Samba V., Diamouangana Z. F. and Mpissi, Loubaki R. (2018). Characterization and Evaluation of the Potential Uses of Mouyondzi Clay. *Journal of Minerals and Materials Characterization and Engineering*, 6, 119-138, https://doi.org/10.4236/jmmce.2018.61010.

11. QGIS (2020). Version AGIS3. 16. [logiciel] système d'information géographique. Disponible sur https://www.agis.org/fr/site/forusers/download.html.

12. Rodríguez-Carvajal, J. (2001). Recent Developments of the Program Full Prof, in commission on Powerder Diffraction (IUCr). 26, 1219.

13. NF P 94-051 NF P 94-052 (1982). European Committee for Standardization, EN 100: Ceramic Tiles- Determination of modulus of rupture. edited by Afnor Paris France.

14. AFNOR NF X 31-107 (1984). Granulats Dans: Recueil des normes françaises du bâtiment et Constituants du béton. Tome 3, 2nd Edn., pp: 78-80.

15. Carignan J., Hild P., Mevelle G., Morel J., Yeghicheyan D. (2001). Routine analyses of Trace elements in geological samples using flow injection and low pressure on-line liquid chromatography coupled to ICP-MS: A study of geochemical reference materials BR, DR-N, UB-N, AN-G and GH. *Geostandards Newsletter*, 25(23), 187-198.

16. Segalen, P**.**, (1971). La détermination du Fer libre dans les sols sesquioxydes. *Cah. O.R.S.T.O.M.*, sér. Pédol., IX(1).

17. Jenroy, E., Guillet, B., Delcroix, P., & Janot, C. (1983). Les formes du fer dans les sols: Confrontation des méthodes chimiques avec la spectrométrie Mössbauer. Bulletin de l'Association française pour l'étude du sol. *Science du sol*, (3-4), 185-194.

18. ISO, N. (1995). 10694: Determination of organic and total carbon after dry combustion (elementary analysis).

19. Rouquerol, F., Luciani, L., Llewellyn, P., Denoyel R. and Rouauerol, J (2003). Texture des matériaux pulvérulents ou poreux. *Editions Techniques de L'Ingenieur*, 2(1050), 1-24

20. Boch, P. (2001). Frittage et microstructures des céramiques: Matériaux et processus céramiques. In: Par Boch P. (Ed.), Paris, Hermès Science Publications, 73-112.

21. Afnor NFX31-130 (1999). Soil-Quality-Chemical Methods-Determination of Cationic Exchange Capacity (CEC) and extractible Cations. Association Francaise de Normalisation.

22. Caillère, S., & Hénin, S. (1964). Minéralogie des argiles. *Soil Science*, 98(3), 208.

23. Javey, C. (1972). Principales matieres premieres utilisees dans l'industrie ceramique.

24. Nkoumbou, C. Villiera, F., Njopwouo, D., Ngoune, G.Y, Barres, O., Pelletier, M., Razafitianamaharavo, A. and Yvon, J. (2008). Physicochemical properties of talc ore from three deposits of Lama Pougue area (Yaoundé Pan-African Belt, Cameroun), in relation to industrial uses. *Applied clay science*, 41(3-4) 113-132.

25. Bertaux, J., Frohlich, F. and Ildefonse, P. (1998). Multicomponment Analysis of FT IR spectra: quantification of amorphe and crystallized mineral phase in synthetique and natural sediments. *Journal of sedimentary Research*, 68(3), 440-447

26. Hmeid, A.H., Akodad, M., Aalaoul, M. and Baghour, M. (2020). Clay mineralogy, chemical and geotechnical characterization of bentonite from Beni Bou Ifrour Massif (the Eastern Rif, Morocco). *Geological Society*, London, February, https://doi.org/10.1144/SP502-2019-25.

27. Rozenson, I. and Heller-kallai, L. (1975). Réduction and oxidation of Fe^{3+} in dioctahedral smectites-III*.Oxidation of octahedral iron in montmorillonite. *Clays and clay Minérals*, 26(2), 88-92.

28. Yvon, J., Baudracco, J., Cases, J.M. and Weiss, J. (1990). Eléments de minéralogie quantitative en microanalyse des argiles. In: Deccareau, A., Ed., Matériaux Argileux, Structures, Propriétés et Applications, SFMC-GFA, Paris, Partie IV, Chap. 3, 473-489.

29. Fayza G.B. (2007). Matériaux de mullite à microstructure organisée composes d'assemblages muscovite – kaolinite. Thèse de doctorat, Université de Limoges.1-243

30. Grosjean, P. (1984). Contribution à la monocuisson rapide de faïence au talc. Etude de pâtes et émaux. Application à l'industrie du carreau de revêtement (suite). L'Industrie céramique (Paris), (780), 106-114.

31. Jouenne C.A. (1990). Traité de céramiques et matériaux minéraux. Editions Septima, Paris. pp 1-657. ISBN: 5552904845010.

32. Casagrande, A. (1948). Classification and Identification of Soils. *Transactions of the American Society of Civil Engineers*, 113(1), 901-930.

33. Fiori C., Fabbri B., Donati, G. and Venturi I. (1989). Mineralogical Composition of the Clay Bodies Used in the Italian Tile Industry. *Applied Clay Science*, 4(5-6), 461-473. https://doi.org/10.1016/0169-1317(89)90023-9.

34. Skempton, A.W. (1953). The colloidal activity of clays. In: Proceedings of the third international. Conference on soil mechanics and foundation engineering. Zurich, Switzerland, August, pp 57-61.

35. Brunauer, S. (1943). The Absorption of the Gases and Vapors L. physical Adsorption. Princeton University Press, Université du Michigan, volume 1, 511p.

36. Mourad F. (2012). Co-adsorption des métaux lourds sur la bentonite modifiée en présence de floculant minéral et biologique. Thèse de Magister, Université de Tizi-ouzou,

37. Van der Weerd J., Heeren R.M.A. and Boon J.J. (2004). Preparation methods and accessories for the infrared spectroscopic analysis of multi-layer paint films. *Studies in Conservation*, 49(3), 193-210, https://doi.org/10.171179/sic.20004.49.3.193.

38. Ayele J., Mahi, A. and Mazet M. (1990). Influence du dodecyl sulfate de sodium sur l'adsorption des acides humiques sur charbon actif en poudre. *Revue des sciences de l'eau*, 3(4), 425-439. https://doi.org/10.7202/705083ar.

39. Nouzha, B. (2007). Elimination du 2-Mercaptonbenzo thiazole par voie photochimique et par adsorption sur la bentonite et le charbon actif en poudre. Magister en chimie, Université Mentouri de Constantine, 1-205

40. Limousin, G., Gaudet, J.P., Charlet, L., Szenknet, S ., Barthese, V. and Krimissa, M. (2007). Sorption isotherms : a review on physical bases modeling and measurement. *Applied geochemistry*, 22(2), 294 -275, https://doi.org/10.1016/j.apgeochem.2006.09.010

41. Zahaf, F. (2017). Etude Structurale des argiles modifiées Appliquées à l'adsorption des pollutants. Thèse de doctorat, Université mustapha stambouli de mascara, p.243.